Int. J. Mach. Tools Manufact. Vol. 33, No. 2, pp. 245–255, 1993.
Printed in Great Britain

0890–6955/93$6.00 + .00

APPLIED MECHANICS IN GRINDING PART II: MODELLING OF ELASTIC MODULUS OF WHEELS AND INTERFACE FORCES

L. C. ZHANG,† TETSUYA SUTO,‡ HOSEI NOGUCHI‡ and TOHRU WAIDA‡

(*Received* 17 *September* 1991; *in final form* 13 *January* 1992)

Abstract—This paper proposes modelling methods of the elastic modulus of grinding wheels and the interface forces over the contact arc between a wheel and a workpiece during grinding operation. It reveals that, for a class of grinding wheels with same types of grain and bond material, the elastic modulus is only a function of dimensionless temperature and a governing non-dimensional variable; interface forces over the grinding contact arc deviate far from the Hertzian profile. The paper produces some useful conclusions for the improvement of grinding technology.

1. INTRODUCTION

IT HAS been claimed again and again by many researchers that interference conditions between a grinding wheel and a workpiece influences very much the surface integrity of the ground components [1–11]. The interference conditions can be characterized by the contact length and the distributions of interface forces [5]. They are essential for the purpose of getting an accurate knowledge of quantitative relationships for the selection of optimal grinding conditions and for the adaptive control or on-line optimization that will increase the productivity of the process by about 20–30%. For example, one direct reason for this is that elastic deflection (as well as thermal expansion) causes the depths of cut to be less than the nominal.

Investigations into the elastic deformation have been performed following experimental and theoretical as well as microscopic and macroscopic approaches. Microscopically, an active grain that removes the chips is deflected because of the forces exerted on it during grinding; macroscopically, the wheel might be considered as a thick circular disc pressed against a curved surface of a workpiece. However, it is just a very rough qualitative picture for understanding a grinding process. It is the fact that the mechanism of elastic deflections, their magnitude and the parameters that influence them are largely a matter of speculation.

Researches before 1980 in this field were well reviewed by Malkin [12] and Saini [6] individually. They concluded that observations concerning the influence of various parameters on the magnitude of contact deflections were diverse from and conflicting with each other and produced a paradox. Specifically, we can summarize them into the following questions:

(1) *What are the effects of wheel grade, grain size and grain type* [9, 13–17]? Some of these researchers claimed significant effects from these factors but some did not agree with these.

(2) Although the contact length has been measured by means of a thermocouple [10, 18–20], an explosive device [9, 21] and various other means, "*what is the correlation of contact length with dominating grinding factors?*" is still an open question. Experimen-

†Dept of Mechanical Engineering, The University of Sydney, NSW 2006, Australia.
‡Machining Technology Division, Manufacturing System Department, Mechanical Engineering Laboratory, 1-2 Namiki, Tsukuba, Ibaraki 305, Japan.

tal observations were very different from theoretical ones [10, 18] (sometimes it was found to be 1.5~2 times the geometrical length but sometimes 1~10 times).

(3) *How does the variation of interface temperature influence contact arc?*

(4) *What are the forms of interface force distributions?*

(5) *What is the dynamic effect on contact length?*

(6) *As a result, what is the importance of the accuracy of contact length and the real shape of the interface to residual stress and temperature distributions?*

Many researchers, e.g. Saini [6, 7], adopted a microscopic approach to investigate the deflection effect. They tried to understand exactly the contact deformation of the grinding wheel by studying the so-called local elastic deflection of a single grain or a small group of grains. There is no doubt that the microscopic approach is useful but how to get the required information from such a method is tricky. Conclusions obtained so far with great efforts are not attractive, and further investigation will be very difficult.

It is important to pay attention to constructing a link between microscopic research and the application of continuum mechanics. A simple method is to ascribe dominating microscopic parameters to some macroscopic factors. It is reasonable to assume, for instance, that the elastic constants of a grinding wheel are functions of temperature, grain size, type of grain and type of bond material; yield stress of workpiece material is a function of temperature. The forms of these functions could be determined by experimental observations. Under such hypotheses, one could expect that results and conclusions deduced from a continuum theory would comprehensively extrapolate to a real case. Several researchers (e.g. Soneys and Wang [22]) did try to solve this problem by continuum mechanics. Unfortunately, they did not very carefully take into account micro-effects and assumed in advance that the pressure distribution over the contact arc was Hertzian. It violated the real circumstance. Although only few experimental results [5] were available due to the difficulties of measuring pressure over the contact bite, they clearly showed that real pressure distribution significantly deviated from Hertzian.

It is the purpose of our research series to discuss the above questions. In this part, we deal with the modelling of the modulus of elasticity of a grinding wheel and the modelling of deformation of a grinding process. It is evident that elastic modulus is a very important parameter in deformation analysis and should be discussed first.

2. MACROSCOPIC MODELLING OF THE ELASTIC MODULUS OF GRINDING WHEELS

2.1. *Analysis*

As has long been realized, the macroscopically measured elastic modulus of a grinding wheel, E, is a physically well defined wheel criterion because it reflects the effects of most microscopic components of the wheel and influences significantly the interface condition between the wheel and the surface under grinding. On the other hand, it could meet the needs of both the manufacturers who should indicate the behaviour of their products and the users who should select a proper wheel for their grinding operations.

People have found that the elastic modulus of a grinding wheel is an extremely complex function of numerous factors: temperature τ; specific weight ρ; hardness grade h_g; concentration c; grain grade G_g; total apparent volume V; volume of grain V_g; volume of bond material V_b; volume of pores V_p; type of grain t_g; type of bond material t_b; and the mean diameter of grains d, that is:

$$E = f(\tau, \rho, c, d, h_g, G_g, t_g, t_b, V, V_g, V_b, V_p) .$$

It seems to be rather difficult to reveal clearly the dependence of E upon these factors. Typical investigations into this problem are those published by Peters *et al.* [23] and

Umino *et al.* [24–30]. The former studied the relations between E and h_g, while the latter discussed the variation of E with c, d, h_g, t_g, V, V_g, V_b and V_p in a series of seven papers and expressed their results by hundreds of curves.

However, it is possible to obtain the nature of E clearly and to simplify the results. We can easily see that hardness grade h_g is determined by τ, d, t_g, t_b, V_g and V_b; concentration c relates to d and V_g; $V_p = V - (V_g + V_b)$; and G_g is equivalent to d. Hence, h_g, c, V_p and G_g are not governing parameters. We could then express E as:

$$E = f(\tau, \rho, d, t_g, t_b, V, V_g, V_b) .$$

Furthermore, for a class of grinding wheels with specific types of grain and bond material, we have:

$$E = f(\tau, \rho, d, V_g, V_b)$$

under a given total apparent volume V. As is evident, the total number of governing parameters, n, is five in the present case. The dimensions of the parameters, for definition in the class MLT, are expressed by the following relations:

$$[E] = FL^{-2}, \quad [\tau] = \theta, \quad [d] = L, \quad [\rho] = FL^{-3}, \quad [V_g] = L^3 \quad \text{and} \quad [V_b] = L^3 .$$

It is easy to see that the first three governing parameters, τ, d and ρ, have independent dimensions so that the number of independent governing parameters, k, is three. According to the well-known Π-theorem, the number of independent dimensionless parameters in the present case is $n - k = 2$, and dimensional analysis gives (see, for example, Sedov [31]):

$$\overline{E} = \Phi(X_1, X_2), \quad X_1 = (\nu_g)^3(\nu_b)(D)^{-3/2}, \quad X_2 = \bar{\tau} \tag{1}$$

where

$$\overline{E} = \frac{E}{d\rho}, \quad \nu_g = \frac{V_g}{V}, \quad \nu_b = \frac{V_b}{V} \quad \text{and} \quad D = \frac{d}{V^{1/3}} .$$

Consequently, according to the above equation, in coordinates $\overline{E} - X_1$, all the experimental points obtained under the same dimensionless temperature, $\bar{\tau}$, should lie on a single curve, if, ideally, there were not any errors in measurement.

2.2. *Illustration and discussion*

As Fig. 1 shows, the above non-dimensional formula (1) is extremely well confirmed. All of the experimental points in Fig. 1 were from the results published by Umino *et al.*

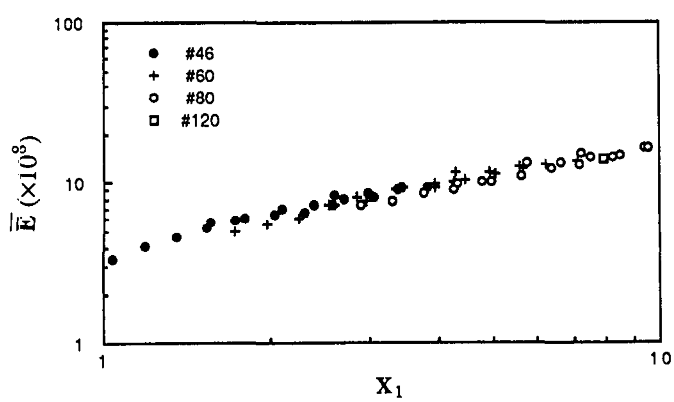

FIG. 1. Non-dimensional elastic modulus.

[26–28], where they expressed these experimental results by 29 individual curves. In obtaining Fig. 1, we have applied the relation of:

$$\rho = \rho_g \nu_g + \rho_b \nu_b$$

where $\rho_g = 39$ (gf cm^{-3}) is the specific weight of the grain and $\rho_b = 24$ (gf cm^{-3}) is that of the bond material. The grinding wheels used here were WA#46V, WA#60V, WA#80V and WA#120V.

Equation (1) is a general relation between non-dimensional Young's modulus $\bar{E}$ and governing factors ν_g, ν_b and D. For different measuring temperatures, different types of grains or different types of bond materials, we obtain different curves. The significance of equation (1) lies in that it reveals the nature of E and that it can hugely reduce experimental work and make theoretical analysis convenient. For example, suppose that we have constructed a curve like that in Fig. 1 using a few experimental data points in the interval $X_1 \in [X_1^{(a)}, X_1^{(b)}]$, then without carrying out any further experiments, we can easily get other E values for those grinding wheels with $X_1 \in [X_1^{(a)}, X_1^{(b)}]$. This curve could also be used to check the correctness and accuracy of the experimental results of grinding wheels with same types of grain and bond material. Those distributed closer to the curve are better; those farther away, worse, or even wrong.

Figure 2 is another illustration. If we add the experimental results from another source [32] into Fig. 1, we can see that they also distribute closely to the single curve, although their wheels were made by different manufacturers. Their wheels were WA#30V, WA#60V, WA#100V and WA#220V.

The non-dimensional elastic modulus $\bar{E}$ implies certain physical meanings. E/ρ relates to the square of the longitudinal wave speed, v, of the material (under the condition of isotropy). Obviously, grain diameter d relates to the anisotropy of the wheel and in turn, influences v. On the other hand, E/ρ is also a measure of specific stiffness which appears in the formula for the bending of beams under their own weight. Fortunately, people are using the methods of sonic test and bending test (e.g. [23,26–28]) to determine modulus of elasticity, although the latter does not presently involve ρ.

The method of the bending test produces the so-called static modulus, E_{stat}, and the method of sonic test gives a dynamic modulus, E_{dyn}. Comparisons [23] showed that these two methods yielded almost the same values of elastic modulus for a specific wheel. Therefore, we shall not distinguish E_{dyn} and E_{stat} in our analysis.

3. A THEORETICAL MODEL TO DETERMINE NORMAL AND TANGENTIAL FORCES

3.1. *Mechanics of grain cutting*

There have been many models proposed over the last decade to describe grain cutting. In these models, three separate forms of grain action are distinguished: rubbing;

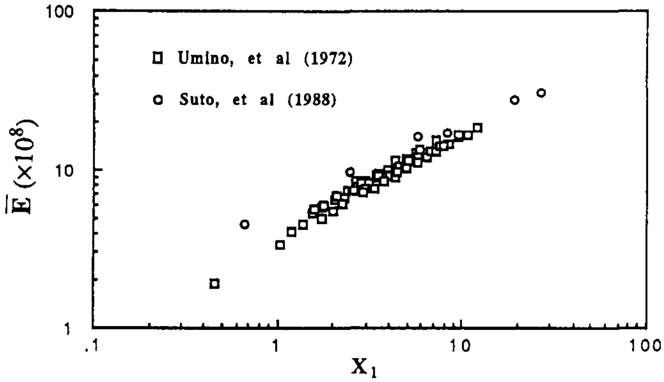

FIG. 2. Comparison of elastic modulus.

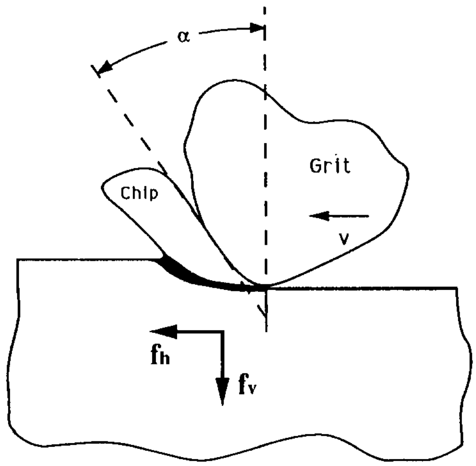

FIG. 3. The cutting process of a mean grain.

ploughing; and cutting. It is very difficult to apply these models to a real abrasive process, since we need in advance to generate an extremely detailed description of the grain's topography in order to determine how much of the grain cuts the workpiece; how much ploughs it and how much rubs it. From the viewpoint of the authors, a simple approach is to propose a model derived from the comprehensive effect of all grains.

The cutting process of a grain should actually be investigated by a three-dimensional model. For the sake of convenience, however, we neglect its transverse effect (in the Z-direction) and focus our attention on the X–Y plane for the time being. During cutting, a grain undergoes a horizontal force, f_h, and vertical force, f_v. The magnitudes of these and the ratio between them mainly depend on cutting speed v and rake angle α of the grain (see Fig. 3); f_h leads to severe plastic shear deformation of the workpiece along its grinding direction and forms a chip; f_v is necessary to keep the depth of cut of the grain, with small α producing small f_v. Usually, the vertical plastic deformation of the workpeice is much smaller than shear deformation. On the other hand, f_h and f_v will yield local elastic deformation of the grain and that of the workpiece surface.

People may think that since the shapes of grains are irregular and the depths of grain cut are different from each other, the distributions of interface forces, normal pressure $p(x)$ and shear force $q(x)$, may be very irregular and even discontinuous (see, for example, the sawtooth curve in Fig. 4). However, we would argue that the wheel and the workpiece are in continuous contact. To a great extent (except randomly distributed active grains), inactive grains, bond material and crammed chips can also be in contact with the workpiece and build up contact forces. Actually and macroscopically, this type of grinding force cannot be distinguished from those of active grains, because they

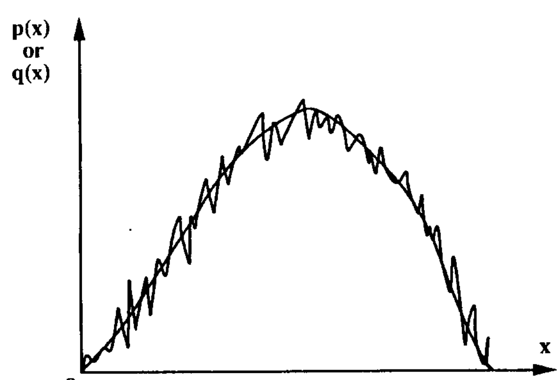

FIG. 4. Smooth and unsmoothed interface forces.

always come together in the chip formation process. Therefore, we can say that $p(x)$ and $q(x)$ can distribute continuously and we can replace the sawtooth curve by a smooth one (Fig. 4).

3.2. *A theoretical model to determine interface forces*

For any steady grinding process with workspeed V_w and depth of wheel cut h, suppose that we observe the movement of the interface by standing on the workpiece. We will then see that the interface boundary shifts forward with V_w but keeps its shape unchanged. Hence (see Fig. 5), let the interface be $f_0(x)$ at instant Γ_0, then at next instant $\Gamma = \Gamma_0 + t$, it shifts to $f_2(x)$. If we remove the grinding wheel at instant Γ, the elastic deformation of the workpiece recovers and we get the instant grinding boundary, $f_1(x)$, after unloading.

Based on the above statement and the discussion on the mechanics of grain cutting in section 3.1, we divide the deformation of the workpiece into two parts (in time interval $[\Gamma_0, \Gamma]$):

(a) The removed part (the part between curves $f_0(x)$ and $f_1(x)$ in Fig. 5): this part of material was cut by active grains, all plastic deformation concentrated in this part; and

(b) The remaining part (the part between curves $f_1(x)$ and $f_2(x)$ in Fig. 5): this part of the material remained owing to the elastic deformation of the workpiece under interface forces.

With the aid of this model, we can calculate the interface forces $p(x)$ and $q(x)$ by contact mechanics. For a given grinding operation, $f_1(x)$ could be obtained from experimental measurement. This determines the initial shape of the workpiece. The grinding wheel is initially cylindrical, it is pushed into contact with the workpiece under a rigid displacement, δ, which makes $x = C_i$ become the first contact point such that we get the nominal depth of cut of the wheel. The term $q(x)$ is simply determined by $\mu p(x)$ where μ is calculated from experimental results.

3.3. *Solution and algorithm*

First, we focus on a conventional grinding problem so that the length of wheel–workpiece interface is much smaller than both the dimension of the wheel and that of the workpiece. The deformation of wheel or workpiece surface can then be approximated by a half plane (plane strain) which is subjected to arbitrarily distributed boundary stresses, $p(x)$ and $q(x)$ (see Fig. 6). This problem could conveniently be solved by the well-known complex function method. Details are shown in the Appendix. Figure 7 is the flow chart of the algorithm for computing $p(x)$ from equations (A.1)–(A.4).

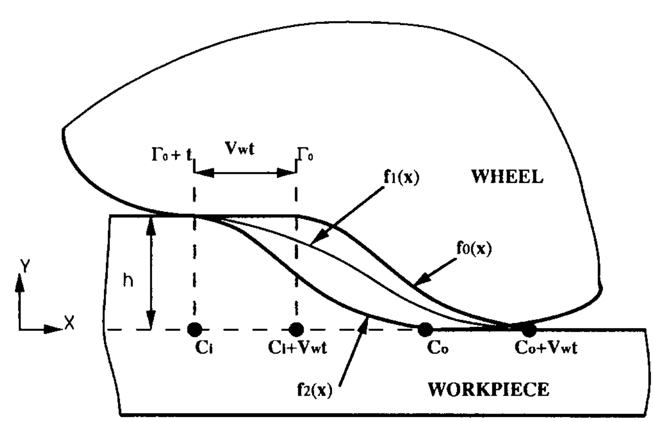

FIG. 5. Theoretical model of the interface state of a grinding process.

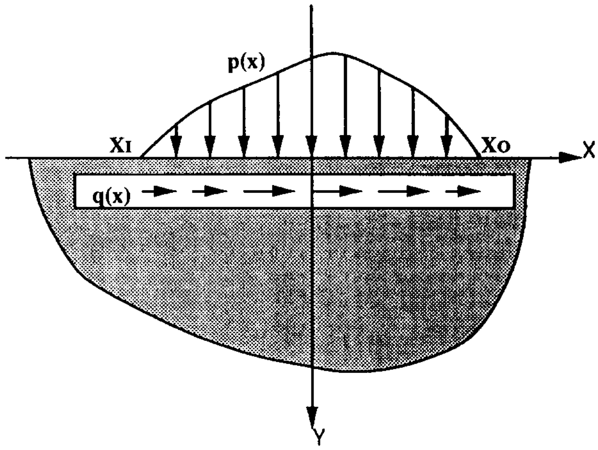

Fig. 6. A half plane subjected to arbitrarily distributed forces.

3.4. *Result and discussion*

As an example, we consider a plough grinding process as investigated experimentally by Okamura *et al.* [5]. The grinding wheel was WA80L9V, its modulus of elasticity is 4×10^4 MPa, Poisson's ratio is 0.2, and diameter is 400 mm. The workpiece is steel SK3, with modulus of elasticity 1.88×10^5 MPa, and Poisson's ratio 0.3. Nominal depth of the wheel cut was 3.8131 μm.

The comparison of theoretical and experimental pressure distributions is shown in Fig. 8. The difference between the two curves is from the approximation of the theoretical model, where we neglected the vertical plastic deformation and ignored the temperature effect.

It is evident that the pressure distribution deviates from Hertzian significantly, because the initial shape of the workpiece surface in steady grinding is not flat. It is different from the contact process of a half plane punched by a long circular cylinder. Hence, to investigate the mechanical residual stresses in ground components, we had better take such a pressure profile as a moving load rather than Hertzian, because it is too rough for simulating a real grinding process. It is quite interesting to notice, like in the case of thin strip rolling, that the shape of the pressure curve is quite similar to that of the temperature curve. The "centre of gravity" of pressure is approximately located at the middle between the inlet contact point and the origin, or the geometrical

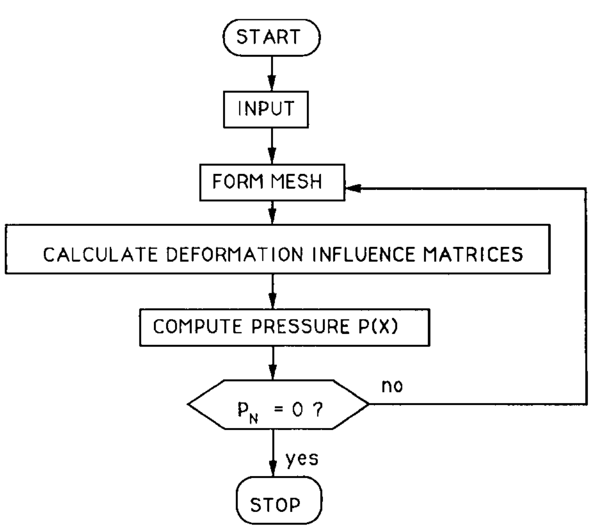

Fig. 7. The flow chart.

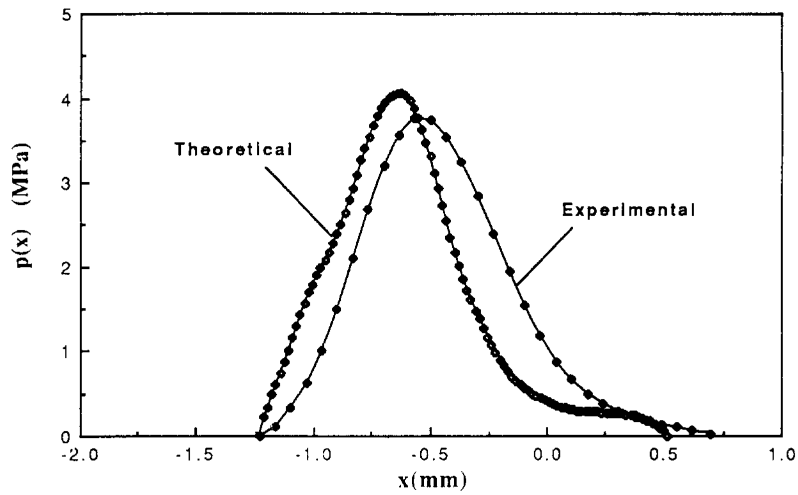

FIG. 8. Pressure distributions (experimental results were from Ref. [5]).

exit contact point. Since the magnitude of $p(x)$ in the region $[0, X_0]$ is small, it is reasonable to think that the resultant forces are applied at the point of $x = X_I/2$. It is useful to grinding engineers. The profile of the interface shear stress, $q(x)$, is similar to $p(x)$ because we applied the relation $q(x) = \mu p(x)$, where μ was determined by experimental data.

Theoretical contact length, l_t, is about 1.42 times longer than the geometrical length, l_g, which is calculated by neglecting elastic deformation of the wheel and workpiece. Theoretical length is smaller than the experimental, l_e, but only by a little ($l_e \approx 1.098 l_t$). This indicates that the factors which we ignored in our theoretical model have no significant effect on the total contact length.

The pressure distribution relates to the variation of chip thickness cut by an individual grain. The variation of chip thickness has been discussed by many researchers (e.g. Hillier [33] and Lindsay [34]). Small chip thickness corresponds to small pressure value. The pressure profile suggests that a lot of rubbing during grinding may occur in the region $[0, X_0]$. This could help in reducing the roughness of the ground surface in certain situations.

Deformation of wheel and workpiece makes the real depth of wheel cut, h, smaller than the nominal depth, h_n, which, in turn, increases the difficulty of controlling the accuracy of the finishing grind. In the present case, $h = 0.938 h_n$.

4. CONCLUSIONS

The paper deals with two important problems in grinding operations. It first finds that the non-dimensional elastic modulus of any given class of grinding wheels is a function of dimensionless temperature $\bar{\tau}$ and a governing non-dimensional variable X_1. This revelation has significant meaning to the development of grinding technology. It can reduce a lot of experimental work, check the correctness and accuracy of experimental results and make theoretical analyses very convenient.

In addition, the paper proposes a simple but realistic theoretical model for calculating interface forces. It shows that actual pressure profiles over the grinding bite greatly deviates from Hertzian pressure. To evaluate mechanical residual stresses, one should apply the fine pressure distribution calculated by the present model. Resultant interface forces are found to exert approximately at the middle of the geometrical contact length ($x = -l_g/2$), which is convenient for grinding engineers to apply in practice.

Further work is needed for the temperature effect on the elastic modulus of the grinding wheels and for a refined model of interface forces by considering vertical plastic deformation.

Acknowledgement—L. C. Zhang would like to thank the Research Development Corporation of Japan for its financial support of his research at MEL in Japan from March 1991 until June 1992.

REFERENCES

[1] R. S. HAHN, The effect of wheel–work conformity in precision grinding, *Trans ASME* **77**, 1325 (1955).
[2] R. S. HAHN and R. LINDSAY, On the effects of real area of contact and normal stress in grinding, *Ann. CIRP* **15**, 179 (1967).
[3] K. V. KUMAR *et al.*, A new method of studying the performance of grinding wheels, *Trans ASME, J. Engng Ind.* **102**, 80 (1980).
[4] K. V. KUMAR and M. C. SHAW, The role of wheel–work deflection in grinding operation, *Trans ASME, J. Engng Ind.* **103**, 73 (1981).
[5] K. OKAMURA *et al.*, Interference condition between grinding wheel and workpiece in plough grinding, *Int. Grinding Conf. Proc.*, Soc. Mfg Engrs, MR84-522, p. 1 (1984).
[6] D. P. SAINI, Elastic deflection in grinding, *Ann. CIRP* **29**, 189 (1980).
[7] D. P. SAINI, Wheel hardness and local elastic deflections in grinding, *Int. J. Mach. Tools Manufact.* **30**, 637 (1990).
[8] E. SALJE *et al.*, Fundamental dependencies upon contact lengths and results in grinding, *Ann. CIRP* **35**, 249 (1986).
[9] W. J. SAUER and M. C. SHAW, The role of elastic deflections of the wheel–work interface in surface grinding, *Int. Conf. on Prod. Engng Procs*, Part 1, p. 645. Tokyo, Japan (1974).
[10] J. VERKERK, The real contact length in cylindrical plough grinding, *Ann. CIRP* **24**, 259 (1975).
[11] J. G. WAGER and D. P. SAINI, Local contact deflections in griding—groups of grains and single grains, *Ann. CIRP* **35**, 245 (1986).
[12] S. MALKIN, ASME review of materials processing literature 1973–1975: Grinding, *Trans ASME, J. Engng Ind.* **99**, 901 (1977).
[13] J. N. BRECKER, Elastic effects in grinding, Ph.D. Thesis, Dept of Mechanical Engineering, Carnegie-Mellon Univ., Pittsburgh, Pennsylvania (1967).
[14] N. P. JEFFRIES, Optimization of grinding processes, in: *New Developments in Grinding* (edited by M. C. SHAW). Carnegie Press, Carnegie-Mellon Univ., Pittsburgh, Pennsylvania (1970).
[15] K. NAKAYAMA, Elastic deformation of contact zone in grinding, *Bull. Jpn Soc. Prec. Engng* **5**, 93 (1971).
[16] K. NAKAYAMA *et al.*, Grinding wheel elasticity, *Trans ASME, J. Engng Ind.* **93**, 609 (1971).
[17] S. H. SALEM and J. K. RUSSELL, Holographic measurement of grinding wheel deformation, *Proc. Int. Conf. on Prod. Engng*, New Dehli, India, Part II, p. VII (1977).
[18] H. MAKINO *et al.*, An experimental investigation of the grinding process, *J. mech. Lab. Japan Eur. Lang. Edn* **12**, 17 (1966).
[19] J. PEKLENIK, Ermittlung von geometrischen und Physicalischen Kenngrossen fur die Grundlagenforschung des Schleifens, Ph.D. Thesis, Auchen, Germany (1957).
[20] H. TSUWA *et al.*, On change of arc of contact length in surface grinding, *J. Jpn Soc. Precis. Engrs* **41**, 358 (1975).
[21] R. H. BROWN and J. D. WATSON, An examination of the wheel–work interface using an explosive device to suddenly interrupt the surface grinding processes, *General Assembly of CIRP*, p. 43 (1977).
[22] R. SONEYS and I.-C. WANG, Analysis of the static and dynamic stiffnesses of the grinding wheel surface, *Proc. 9th Int. Conf. MTDR*, p. 1133. Manchester, England. Pergamon Press (1968).
[23] J. PETERS, R. SNOEYS and A. DECNEUT, Sonic testing of grinding wheels, *Proc. 9th Int. Conf. MTDR*, Manchester, England. Pergamon Press (1968).
[24] K. UMINO and N. SHINOZAKI, Ultrasonic velocity in grinding wheel—study on grinding wheels by ultrasonic pulse method, Part I, *J. Jpn Soc. Precis. Engrs* **36**, 538 (1970).
[25] K. UMINO and N. SHINOZAKI, Dynamic elastic modulus of griding wheel—study on grinding wheels by ultrasonic pulse method, Part II, *J. Jpn Soc. Precis. Engrs* **36**, 608 (1970).
[26] K. UMINO, R. YAMANAKA and N. SHINOZAKI, On the estimation of grade of fine-grain-size grinding wheel—study on grinding wheels by ultrasonic pulse method, Part III, *J. Jpn Soc. Precis. Engrs* **38**, 161 (1972).
[27] K. UMINO and N. SHINOZAKI, Elastic modulus and bending strength of grinding wheel—study on grinding wheels by ultrasonic pulse method, Part IV, *J. Jpn Soc. Precis. Engrs* **38**, 349 (1972).
[28] K. UMINO and N. SHINOZAKI, New grade tester of grinding wheel using ultrasonic pulse method—study on grading of grinding wheels by ultrasonic pulse method, Part V, *J. Jpn Soc. Precis. Engrs* **38**, 485 (1972).
[29] K. UMINO, S. TOOE and N. SHINOZAKI, Study on irregularity of wheel grade, Part I—irregularity of wheel grade and grinding phenomenon, *J. Jpn Soc. Precis. Engrs* **49**, 741 (1983).
[30] K. UMINO, S. TOOE and N. SHINOZAKI, Study on irregularity of wheel grade, Part II—detection of irregularity of wheel grade by dressing resistance method, *J. Jpn Soc. Precis. Engrs* **49**, 1416 (1983).
[31] L. I. SEDOV, *Similarity and Dimensional Methods in Mechanics*. Academic Press, London (1959).
[32] T. SUTO *et al.*, Performance and quality comparison of grinding wheels made in Japan and Korea, *J. Jpn Soc. Grinding Engrs* **32**, 30 (1988).
[33] M. J. HILLIER, On a three-dimensional model of the surface griding process, *Int. J. Mach. Tool Des. Res.* **6**, 109 (1966).
[34] R. P. LINDSAY, On the surface finish–metal removal relationship in precision grinding, *ASME Winter Annual Meeting*, New York (1972).
[35] N. I. MUSKHELISHVILI, *Some Basic Problem of the Mathematical Theory of Elasticity*. Nauka, Moscow (Translation of an earlier edition published by Noordhoff, Groningen, 1953) (1966).

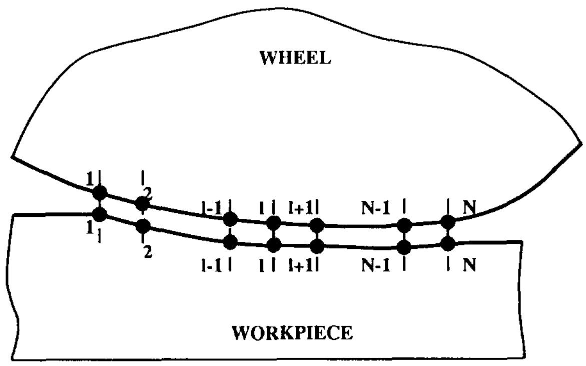

FIG. A.1. Pairs of contact nodes on interfaces.

APPENDIX

Complex function method in the theory of elasticity [35] gives:

$$2G^{(k)}(u^{(k)} + iv^{(k)}) = (3 - 4\nu^{(k)})\Omega(z) + \Omega(\bar{z}) + (\bar{z} - z)\overline{\Omega'(z)} \quad \text{(A.1a)}$$

$$\sigma_x^{(k)} + \sigma_y^{(k)} = 2\{\overline{\Omega'(z)} + \Omega'(z)\} \quad \text{(A.1b)}$$

and

$$\sigma_y^{(k)} - i\tau_{xy}^{(k)} = \Omega'(z) - \Omega'(\bar{z}) + (z - \bar{z})\overline{\Omega''(z)} \quad \text{(A.1c)}$$

where

$$G^{(k)} = \frac{E^{(k)}}{2(1 + \nu^{(k)})}, \quad z = x + iy, \quad \bar{z} = x - iy, \quad i = \sqrt{-1}$$

superscript $k = 1$ or 2 indicates wheel or workpiece, respectively, u and v are displacement components in the x and y directions, σ_x, σ_y and τ_{xy} are stress components. Stress boundary condition is

$$\sigma_y^{(k)} - i\tau_{xy}^{(k)} = -p(x)[1 + i\mu] \quad \text{on} \quad y = 0\,.$$

Hence,

$$\Omega'(z) = -\frac{1}{2\pi i}\int_{-\infty}^{+\infty} \frac{p(t) + iq(t)}{t - z}\,\mathrm{d}t = \frac{-\mu + i}{2\pi}\int_{x_1}^{x_0} \frac{p(t)}{t - z}\,\mathrm{d}t\,. \quad \text{(A.2a)}$$

If we divide the grinding contact arc into n small elements (Fig. A.1) and assume that $p(x)$ is linearly distributed over an element $j\{x \in [x_j, x_{j+1}]\ (j = 1, \ldots, n)\}$ (Fig. A.2), we get an explicit expression for $\Omega'(z)$ in $[x_j, x_{j+1}]$:

$$\Omega_j'(z) = \frac{-\mu + i}{2\pi}\left\{c_1 L + (c_2 + c_1 z)\ln\left(\frac{x_{j+1} - z}{x_j - z}\right)\right\} \quad \text{(A.2b)}$$

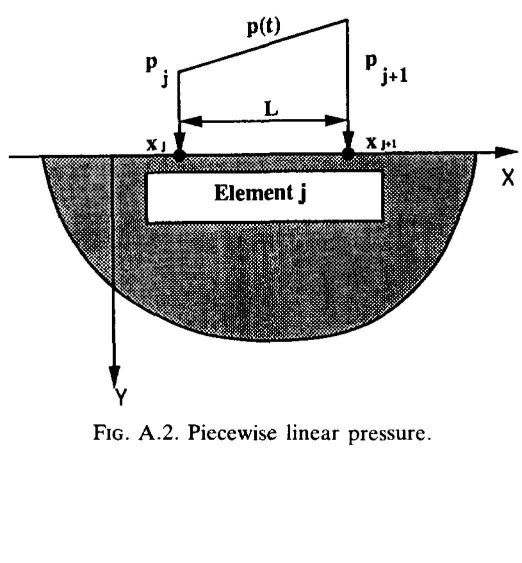

FIG. A.2. Piecewise linear pressure.

where

$$c_1 = \frac{p_{j+1} - p_j}{L}, \quad c_2 = \frac{p_j x_{j+1} - p_{j+1} x_j}{L}, \quad L = x_{j+1} - x_j$$

and subscript j stands for element j.

The normal displacement at node point l is then determined by:

$$v_l^{(k)} = C_{lm}^{(k)} p_m + D_{lm}^{(k)} q_m, \quad (l = 1, \ldots, N) \tag{A.3}$$

where $C_{lm}^{(k)}$ and $D_{lm}^{(k)}$ are deformation influence matrices which are derived from equations (A.1) and (A.2). Repeated subscripts indicate a summation from 1 to N, N being the total node number. Compatibility condition of normal displacements of wheel and workpiece at point $l(l=1, \ldots, N)$ leads to the equations for determining pressure $p(x)$, that is:

$$\{C_{lm}^{(1)} + C_{lm}^{(2)} \pm \mu(D_{lm}^{(1)} + D_{lm}^{(2)})\} p_m = H_l, \quad (l=1, \ldots, N) \tag{A.4}$$

where H_l is the difference between $F_2(x)$ and $F_1(x)$ at node l, $F_k(x) = h - f_k(x)$ $(k = 1, 2)$, and $\pm$ corresponds to the rotating direction of the grinding wheel.